ECS Transactions, 78 (1) 1407-1416 (2017) 10.1149/07801.1407ecst ©The Electrochemical Society

Nanostructured SOFC Electrode Scaffolds Prepared via High Temperature in situ Carbon Templating of Hybrid Materials

S. P. Muhoza^a, T. E. Barrett^a, S. E. Soll^a, and M. D. Gross^{a, b}

^a Department of Chemistry, Wake Forest University, Winston-Salem, NC 27109, USA
^b Center for Energy, Environment, and Sustainability, Wake Forest University, Winston-Salem, NC 27109, USA

High surface area solid oxide fuel cell (SOFC) electrode scaffold materials were prepared at traditional sintering temperatures by sintering hybrid inorganic-organic gels in argon. The prepared materials were yttria-stabilized zirconia (YSZ, 8 mol% Y₂O₃), gadolinia doped ceria (GDC, Ce_{0.8}Gd_{0.2}O_{3-δ}) and strontium titanate (STO, SrTiO₃). Gels were prepared via the citric acid (Pechini) method and the propylene oxide method. The gels were sintered between 1050°C and 1350°C in argon, creating an amorphous carbon template in situ, which preserved a ceramic scaffold nanostructure. The carbon template was removed upon heating in air to 700°C. Specific surface areas up to 83, 95, and 99 m²/g were achieved for YSZ, GDC, and STO, respectively. The carbon template concentration and resulting surface areas are tunable by modifying the gel formulations. Symmetric cathode cells were prepared with traditional and nanostructured YSZ. As expected, the gel-derived, nanostructured YSZ improved electrode performance.

Introduction

Lowering the operating temperature of solid oxide fuel cells (SOFCs) to the 300°C-600°C range has been the main goal for many researchers. Low temperature SOFCs are not only advantageous for conventional SOFC applications such as stationary power generation, but they are also viable for others such as portable, transportation, electrolytic and energy storage applications (1). However, lowering the operating temperature results in significant activation losses due to slow electrode kinetics (2).

Two of the most effective ways to address challenges arising with low-temperature SOFC performance include: 1) increasing the density of electrochemically active sites in the porous electrodes and 2) adopting new material sets with higher electrocatalytic activities. These two solutions can be achieved with the *in situ* carbon templating processing method reported in this study. With this method, high surface area materials, up to $100 \text{ m}^2 \cdot \text{g}^{-1}$, are prepared at traditional sintering temperatures and these can be incorporated in fuel cell electrodes to increase the density of electrochemical active sites (3). Moreover, this work demonstrates that our method is applicable to three different mixed-metal-oxide materials and two different types of hybrid inorganic-organic materials. Thus, it is likely that this method can be used to prepare newly discovered material sets with improved electrocatalytic activity.

The *in situ* carbon templating method reported in this work consists of sintering a hybrid inorganic-organic material in flowing argon at traditional sintering temperatures (1000°C-1400°C). During the sintering process, a hard amorphous carbon template is formed and this template preserves the scaffold's nanostructure. High surface area ceramic materials are obtained by heating the sintered material in air at 700°C, which completely removes the carbon template by oxidation. In our previous work, we demonstrated that YSZ with up to 200 times higher surface area than traditional methods can be created via *in situ* carbon templating of a hybrid inorganic-organic propylene oxide (PO) gels (4,5). In this study, we show that GDC, STO, and YSZ with essentially the same high surface area can also be prepared via *in situ* carbon templating of both PO gels and citric acid gels.

All the materials prepared in this work were sintered between 1050°C and 1350°C, practical temperatures for SOFC electrode fabrication. Thus, this method can be used to prepare high surface area electrode scaffolds. This is vital to SOFC electrode design research as, although the surface area of scaffold materials essentially dictates the ultimate electrode performance (6), little progress has been made to increase the surface area of the porous ceramic scaffold itself. One great feature of the *in situ* carbon templating method is its tunability. The carbon template concentration and the final surface area can be systematically controlled by adjusting the concentration of the organic component in the hybrid material. Such tunability enables a high degree of flexibility for optimizing electrode performance. Practical use of these materials in low temperature SOFC electrodes is further discussed.

Experimental

Hybrid Inorganic-Organic Gel Preparation

The hybrid gel formulations were designed to ultimately produce nanostructured ceramics of yttria stabilized zirconia (YSZ, 8 mol% Y₂O₃), gadolinia doped ceria (GDC, Ce_{0.8}Gd_{0.2}O_{3-δ}), and strontium titanate (STO, SrTiO₃).

The synthesis of propylene oxide gels containing Zr and Y has been previously reported in detail (4,5). ZrCl₄ (99.5+%, Alfa Aesar) and Y(NO₃)₃·6H₂O (99.9%, Alfa Aesar) were dissolved in deionized water in a Zr:Y:H₂O molar ratio of 5.75:1:650 with magnetic stirring. Glucose (≥ 99.9%, Alfa Aesar) was then dissolved in the solution in three glucose:total metals molar ratios: 0:1, 2.5:1, and 5:1. Propylene oxide (PO, ≥ 99.5%, Sigma-Aldrich) was then added to the solution in a PO:total metals molar ratio of 10:1 and stirred for several seconds to initiate the gelation reaction. The gel formed within a few minutes. These gels are referred to as YSZ-PO. Propylene oxide gels containing Ce and Gd were prepared by dissolving CeCl₃·7H₂O (99%, Alfa Aesar) and GdCl₃·6H₂O (99%, Sigma-Aldrich) in an 80°C mixture of ethanol (EtOH) and deionized water in a Ce:Gd:EtOH:H₂O molar ratio of 4:1:475:475. Glucose was dissolved and then PO was added to the solution. The temperature was then increased to 95°C and mechanical stirring was maintained for many hours until gel formation. These gels are referred to as GDC-PO.

Citric acid gels containing Zr and Y were synthesized by dissolving ZrCl₄, YCl₃ (99.9%, Alfa Aesar), citric acid (CA, 99+%, Alfa Aesar), and ethylene glycol (EG, >99.75%, Acros Organics) in deionized water. The Zr:Y:H₂O molar ratio was 5.75:1:1150.

Citric acid gels containing Ce and Gd were similarly prepared using CeCl₃·7H₂O and GdCl₃·6H₂O with a Ce:Gd:H₂O molar ratio of 4:1:850. In both cases, three CA:EG:total metals molar ratios were used: 1:1:1, 5:5:1, and 10:10:1. The mixtures were heated to 80°C with mechanical stirring until gel formation. These gels are referred to as YSZ-CA and GDC-CA.

Citric acid gels containing Sr and Ti were prepared using $SrCl_2 \cdot 6H_2O$ (99+%, Alfa Aesar) and TiCl₃ solution (\geq 12%, Sigma-Aldrich) in a 1:1 Sr:Ti molar ratio. TiCl₃, ethylene glycol, and citric acid were mixed with magnetic stirring and heated to 60°C for 10 minutes. $SrCl_2$ was then added to the mixture and the temperature was raised to 80°C. The mixture was stirred until gel formation. These gels are referred to as STO-CA.

Gels were sintered in a tube furnace under flowing argon with the following temperature program: ramp from ambient temperature to 850°C at a rate of 5°C/min, ramp from 850°C to the sintering temperature at a rate of 2°C/min, hold at the sintering temperature for 2 h, and cool to ambient temperature with the same respective ramp rates. All gels were sintered at 1050°C. Additionally, propylene oxide gels with a glucose:total metals molar ratio of 5:1 and citric acid gels with a CA:EG:total metals molar ratio of 10:10:1 were sintered at 1150°C, 1250°C, and 1350°C. In all cases, the samples were black upon sintering due to the formation of an amorphous carbon template *in situ*. Subsequently, samples were heated in air at 700°C for 2 h to remove the carbon template.

Materials Characterization

Powder x-ray diffraction (XRD) patterns were collected with a Bruker D2 Phaser x-ray diffractometer using CuKα radiation for a 2θ range of 20° to 80° with a 0.02° increment and a 0.2 s time step. The stage was rotated one revolution per minute. Thermogravimetric analysis (TGA) was completed using a TA Instruments SDT Q600 to determine the carbon template concentration (4). Samples were heated from ambient temperature to 1200°C at a ramp rate of 10°C·min⁻¹ in air flowing at a rate of 100 mL·min⁻¹. Brunauer, Emmett, and Teller (BET) surface areas were determined using a Micromeritics Tristar II 3020 surface area analyzer. Samples were degassed at 250°C for 2 h under flowing nitrogen prior to testing. All surface area measurements were completed with N₂ adsorption at 77K and all reported surface areas had a correlation coefficient of at least 0.9995.

Symmetrical Cell Fabrication

Symmetrical cells were fabricated by laminating together three tape-casted films followed by sintering in air at 1500° C for 4 h. The middle layer was a YSZ (8 mol% Y_2O_3) film from ESL ElectroScience and the outer films contained YSZ (8 mol% Y_2O_3 , Tosoh) particles and graphite pore formers (325 mesh, Alfa Aesar) (7). Sintering resulted in the following symmetrical cell dimensions: 100 µm thick YSZ electrolyte with a cross sectional area of 1.8 cm², symmetric 50 µm thick porous YSZ layers with a cross sectional area of 0.38 cm², and ~65% porosity.

Symmetrical cells were infiltrated with YSZ-PO solution to saturation (prior to gelation) with a glucose:total metals molar ratio of 5:1. The cell was sintered in flowing argon at 1050° C for 2 h followed by heating in air to 700° C for 2 h. The nanostructured YSZ derived from the YSZ-PO gel was ~2.5 vol% of the electrode. The porous YSZ

scaffolds were subsequently infiltrated with a 0.7M aqueous solution containing La(NO₃)₃·6H₂O (99.9%, Alfa Aesar), Sr(NO₃)₂ (99%, Alfa Aesar), Fe(NO₃)₃·9H₂O (98+%, Alfa Aesar), and citric acid in a molar ratio of 0.8:0.2:1:2. Multiple infiltrations were required to achieve a La_{0.8}Sr_{0.2}FeO_{3-δ} (LSF) loading of ~26 vol% of the electrode. After each infiltration, the cell was heated in air to 450°C. After completion of all infiltration steps, the cell was heated in air to 850°C for 2 h to form the LSF phase. Symmetrical LSF-YSZ cells were also fabricated with the same procedure except that no gel was infiltrated into the scaffold.

Symmetrical Cell Electrochemical Characterization

Electrical contacts were made at both LSF-YSZ electrodes with Ag wire and Ag ink. The cell was held at 550°C in air during testing. Electrochemical impedance spectra were collected using a Gamry Instruments Series G750 potentiostat with four probes in the galvanostatic mode at a dc current of 0 mA with an ac perturbation of 5 mA over a frequency range of 10⁵ Hz to 10⁻¹ Hz. The ohmic contributions were subtracted from the impedance and the non-ohmic impedance was multiplied by 0.5 since both electrodes contribute to the impedance.

Results

Figure 1a shows XRD patterns of the YSZ-PO, YSZ-CA, GDC-PO, GDC-CA, and STO-CA gels sintered in argon at 1050°C for 2 h. The glucose:total metals molar ratio was 5:1 for the PO gels and the CA:EG:total metals molar ratio was 10:10:1 for the CA gels. Both YSZ gel patterns have broad peaks that match the Zr_{0.84}Y_{0.16}O_{1.92} standard pattern, and the STO-CA pattern has broad peaks that match the SrTiO₃ standard pattern. The GDC-CA pattern has the broadest peaks and the only prominent peak corresponds to the highest intensity peak of the Gd_{0.2}Ce_{0.8}O_{1.9} standard pattern at a 2θ of 28.48°. The GDC-PO pattern, however, shows several sharp peaks that correspond to Gd_xCe_{1-x}OCl. To investigate whether the oxychloride phase formed during gel synthesis or sintering in argon, an XRD pattern of the as-prepared GDC-PO gel was collected. The as-prepared pattern did not contain the oxychloride peaks, indicating that this phase formed upon sintering.

As will be discussed and shown in Table 1, the samples represented in Figure 1 comprise 78-85 vol% carbon. The lack of any crystalline carbon peaks in the XRD patterns suggests that the hard carbon template formed *in situ* during sintering is amorphous. The formation of amorphous carbon is consistent with the observation that the carbon template is completely removed by oxidation in air below 700°C.

Figure 1b shows XRD patterns of YSZ-PO, YSZ-CA, GDC-PO, GDC-CA, and STO-CA gels that were sintered in argon at 1050°C for 2 h and subsequently heated in air at 700°C for 2 h. In all cases, the peaks correspond to the pure, desired mixed-metal-oxide phase. In addition, all the peaks are broad and correspond to crystallite sizes in the 6-10 nm range, as estimated using the Scherrer equation. Figure 2 shows XRD patterns of the same gels sintered in argon at 1350°C for 2 h and subsequently heated in air at 700°C. For GDC-PO, a small Gd₂O₃ peak is observed at a 2θ of 29.1°. This suggests that a small amount of Gd may have phase separated from Ce during sintering at 1350°C.

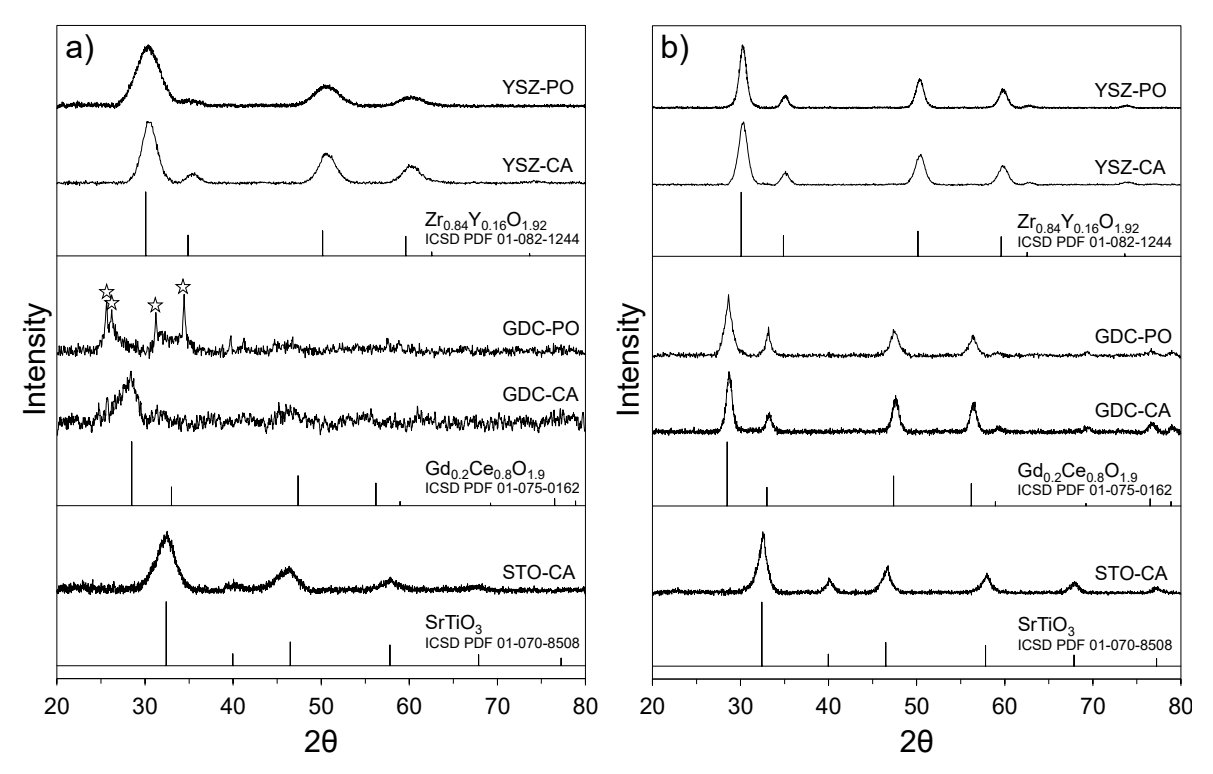


Figure 1. X-ray diffraction patterns of PO gels and CA gels a) sintered in argon at 1050° C for 2 h and b) sintered in argon at 1050° C for 2 h followed by heating in air at 700° C for 2 h. \Rightarrow = Gd_xCe_{1-x}OCl

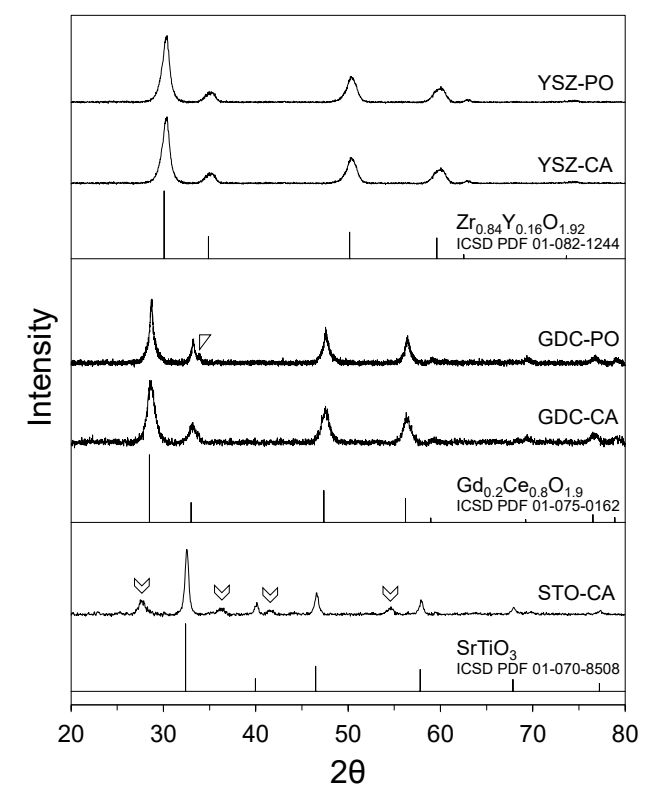


Figure 2. X-ray diffraction patterns of PO gels and CA gels sintered in argon at 1350°C for 2 h followed by heating in air at 700°C for 2 h. $\nabla = \text{Gd}_2\text{O}_3$, $\bowtie = \text{TiO}_2$.

To further investigate, the XRD pattern of GDC-PO sintered in argon at 1350°C for 2 h was analyzed; however, no impurity peaks were observed. Perhaps the peaks were too broad to observe the presence of any impurity peaks. It is possible that a small Gd₂O₃ peak may also be present in the GDC-CA pattern in Figure 2, however the peak is too broad to make this determination. The STO-CA pattern in Figure 2 shows several impurity peaks that correspond to TiO₂. While not shown here, TiC impurity peaks were observed in the XRD pattern of the STO-CA gel sintered in argon at 1350°C. Thus, the formation of a TiC phase likely caused a sufficient degree of separation between Sr and Ti atoms such that heating to 700°C was not enough thermal energy to form the pure SrTiO₃ phase. The samples represented in Figure 2 had crystallite sizes in the 8-16 nm range, as estimated using the Scherrer equation

Table 1 shows carbon template concentration as a function of organic:total metals molar ratio for CA and PO gels sintered in argon at 1050°C for 2 h. The concentration of organic content in the CA gel was systematically varied by adjusting the CA and EG concentrations. The concentration of organic content in the PO gel was systematically varied by adjusting the glucose concentration. The carbon template concentration was determined using TGA as described elsewhere (4). Perhaps most importantly, the carbon template concentration increased with an increase in organic content for all gel formulations, demonstrating that the carbon template concentration can be systematically controlled. As shown in Table 1, adjusting the STO-CA gel formulation allowed the carbon template concentration to be varied between approximately 40 vol% and 80 vol% of the mixed-metal-oxide/carbon template composite. For YSZ-CA and GDC-CA, the carbon template concentration was varied between about 50 vol% and 80 vol%. The PO gels allowed for more flexibility in the carbon template concentration at the lower end of the range. With no glucose in the PO gel formulation, the YSZ-PO and GDC-PO carbon template concentrations were 10 vol% and 29 vol%, respectively. The highest glucose concentration resulted in 80 vol% and 85 vol% carbon template for YSZ-PO and GDC-PO, respectively.

Table 1. Carbon template concentration as a function of gel formulation. Concentration is shown as vol% of the sintered mixed-metal-oxide/carbon template composite. The hybrid materials were sintered in argon at 1050°C for 2 h.

	CA:EG:M (Citric Acid Gel)			Glucose:M (Propylene Oxide Gel)		
_	1:1:1	5:5:1	10:10:1	0:1	2.5:1	5:1
YSZ	50	57	78	10	44	80
GDC	51	69	78	29	68	85
STO	39	66	80			

The mixed-metal-oxide/carbon template composites represented in Table 1 were heated in air at 700°C for 2 h to remove the carbon template by oxidation, and the BET surface areas of the resulting mixed-metal-oxides are shown in Table 2. In all cases, surface area increased with an increase in organic content, and the corresponding increase in carbon template concentration. The results demonstrate that the mixed-metal-oxide surface area can be systematically controlled between roughly 10 m²·g⁻¹ and 100 m²·g⁻¹ when

sintered in argon at 1050°C. If one assumes spherical particles of equal size, these surface areas correspond to particle sizes of 100 nm and 10 nm, respectively.

Table 2. Ceramic BET specific surface area, in m²·g⁻¹, as a function of gel formulation. The samples were sintered in argon at 1050°C for 2 h and then heated in air at 700°C for 2 h.

	CA:EG:M (Citric Acid Gel)			Glucose:M (Propylene Oxide Gel)		
_	1:1:1	5:5:1	10:10:1	0:1	2.5:1	5:1
YSZ	36	55	83	14	46	82
GDC	33	39	61	16	75	91
STO	12	65	99			

The effect of sintering temperature on the final ceramic surface area was investigated by sintering CA gels with a CA:EG:total metals molar ratio of 10:10:1 and PO gels with a glucose:total metals molar ratio of 5:1 in argon at 1050°C, 1150°C, 1250°C, and 1350°C for 2 h. As shown in Figure 3, the surface areas are generally highest for 1050°C and decrease with increasing sintering temperature. In some cases, the surface area for 1150°C is slightly higher than for 1050°C, but from a particle size standpoint these surface areas are virtually the same. A sharp decrease in surface area was observed for STO-CA when the sintering temperature was increased from 1050°C to 1150°C. It is unclear why the decrease is sharp, but perhaps it is related to the formation of a TiC impurity phase, which is known to form somewhere between 1150°C and 1250°C via XRD results. Most importantly, surface areas between 40 m²·g⁻¹ and 60 m²·g⁻¹ were achieved even after

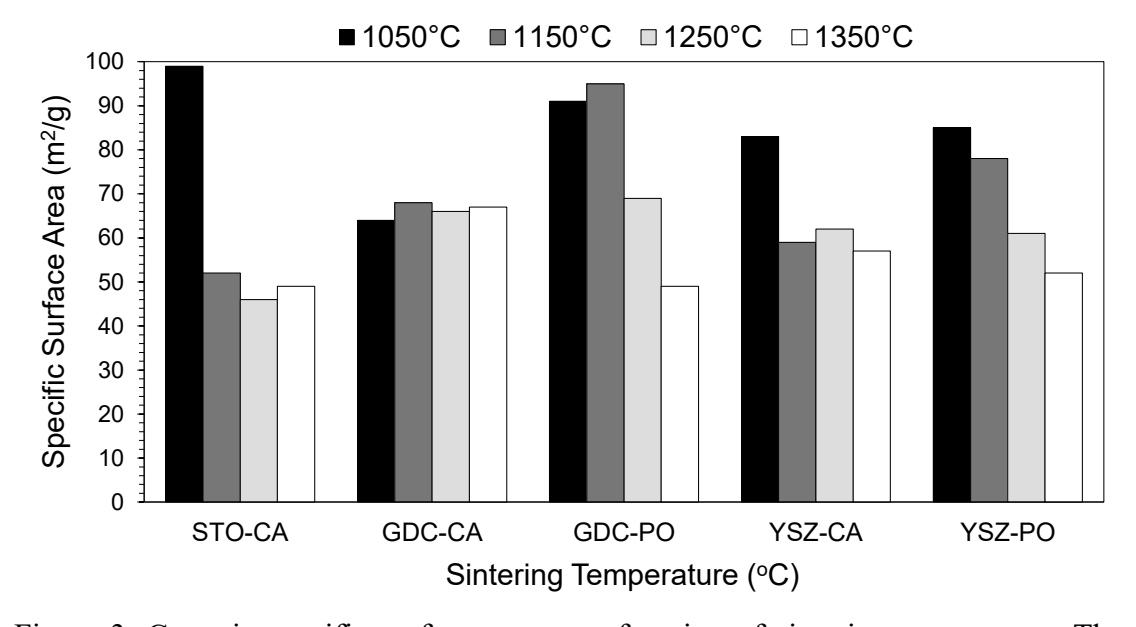


Figure 3. Ceramic specific surface area as a function of sintering temperature. The samples were sintered in argon at the indicated sintering temperature for 2 h and then heated in air at 700°C for 2 h.

sintering at 1350°C. This is an outstanding result considering traditional YSZ scaffold surface areas are typically 0.5-1 m²·g⁻¹ when sintered at this temperature.

The goal of developing these nanostructured mixed-metal-oxides is to improve the performance of SOFCs at low temperature. As proof of concept, YSZ-PO with a glucose:total metals molar ratio of 5:1 was infiltrated into a symmetrical cell containing porous YSZ electrode scaffolds. Subsequently, the porous scaffolds were infiltrated with LSF. For comparison, a similar LSF-YSZ symmetrical cell with no infiltrated YSZ-PO gel was prepared. Electrochemical impedance spectra of symmetrical cells with and without the nanostructured YSZ are shown in Figure 4. The impedance spectra were collected at 550°C in air. The non-ohmic electrode resistance, obtained from the low frequency abscissa of the Cole-Cole plot, was $3.15 \,\Omega \cdot \mathrm{cm}^2$ for the traditional symmetrical cell. When nanostructured YSZ was incorporated into the electrodes by YSZ-PO gel infiltration, the non-ohmic electrode resistance decreased to $1.75 \,\Omega \cdot \mathrm{cm}^2$; a 44% improvement in electrode performance. Clearly, the incorporation of gel-derived nanostructured mixed-metal-oxides can dramatically improve electrode performance.

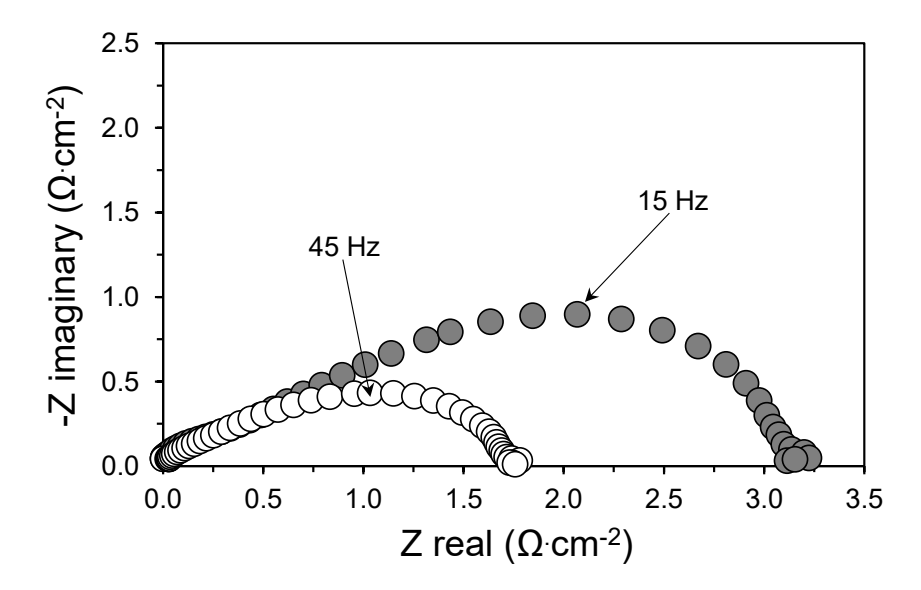


Figure 4. Electrochemical impedance spectra of LSF-YSZ symmetrical cells with traditional YSZ scaffolds (and traditional YSZ scaffolds infiltrated with a YSZ-propylene oxide gel with a glucose: M of 5:1 (). After gel infiltration, the scaffolds were sintered in argon at 1050°C for 2 h and then heated in air at 700°C for 2 h.

Discussion

In previous work, we have shown that high surface area YSZ can be prepared via *in situ* carbon templating of PO gels (4,5). In the current work, it has been shown that the same approach can be used to prepare high surface area fuel cell materials beyond YSZ. This work also demonstrates that the general *in situ* carbon templating approach is feasible using other hybrid inorganic-organic materials, and that one can systematically tune the carbon template concentration and resulting surface area.

A potential limitation of the *in situ* carbon templating approach is that a metal carbide phase may form during sintering in an argon atmosphere, resulting in the formation of an impurity metal oxide phase during removal of the carbon template by oxidation at 700°C. In the current work this was observed for STO-CA sintered at 1350°C. After sintering STO-CA at 1350°C, XRD showed that TiC was the dominate phase and SrTiO₃ was only present as a minor phase. Upon oxidation at 700°C, SrTiO₃ was the dominate phase and a significant TiO₂ impurity phase was also present. For STO-CA sintered at 1250°C in argon, TiC and SrTiO₃ phases were about equally present; however, no TiO₂ impurity was present after oxidation at 700°C. For STO-CA sintered at 1150°C and 1050°C in argon, no TiC phase was observed.

Similar behavior was observed for both YSZ gels in that a ZrC phase was increasingly present as the sintering temperature in argon was increased from 1150°C to 1350°C. Upon oxidation at 700°C, however, a pure YSZ phase was observed by XRD for all sintering temperatures. For both GDC gels, no metal carbide phase was detected even at 1350°C.

The presence of impurity metal oxide phases can be deleterious to the desired material functionality. For example, doped SrTiO₃ is often used as an electronic conductor in SOFC electrodes, but TiO₂ is an electronically insulating phase. YSZ is an excellent oxygen ion conductor, but monoclinic ZrO₂ is an oxygen ion insulator. We are currently exploring strategies to avoid carbide formation during *in situ* carbon templating sintering. One strategy is to replace the inert argon sintering atmosphere with a low oxygen fugacity atmosphere. The idea is to create a high enough oxygen fugacity that the metal carbide phase is not thermodynamically favorable, but low enough that the carbon template does not oxidize to CO or CO₂ during sintering. Preliminary results suggest this is a promising approach.

Finally, with the feasibility of the *in situ* carbon templating approach established for relevant SOFC materials, one can start thinking about how to incorporate these materials into electrodes. As a first attempt, we simply infiltrated YSZ hybrid material into a traditional YSZ scaffold, and the electrode performance improvement at low temperature was dramatic. It is reasonable to expect that optimizing this approach would garner further performance improvements. Infiltrating GDC and STO hybrid materials into scaffolds has not been explored yet. Beyond infiltration into existing scaffolds, the hybrid materials could be directly mixed with traditional scaffold particles and pore formers in the scaffold formulation. There is great flexibility in how this could be done. The as-prepared hybrid gel or the sintered mixed-metal-oxide/carbon composite powder could be used. The carbon template concentration, sintering temperature, and the composition of the nanostructured ceramic, larger traditional ceramic particles, and pore formers can all be varied over a wide range of values.

Conclusion

High surface area ceramic scaffold materials were prepared via *in situ* carbon templating of hybrid materials. Two different types of hybrid materials were used and three different types of ceramic materials relevant to SOFCs were prepared. During sintering, a hard carbon template was formed and its concentration was systematically tuned. Surface areas over 80 times higher than current scaffold materials were achieved after heating in

air at 700°C for 2 h. This implies that these materials have great thermal stability at low-temperature (~500°C) and, hence, should improve the performance of SOFC operating at such a temperature. This was confirmed by our symmetrical cell performance tests in which the cell incorporated with our high surface area material showed a 44% performance improvement compared to the traditional cell. Further investigation on the process optimization could enable substantial improvements in low temperature cell performance.

Acknowledgements

This work was supported by the Wake Forest Chemistry Department, the Wake Forest Center for Energy, Environment, and Sustainability (CEES), and the National Science Foundation Faculty Early Career Development Program (CAREER) award (CMMI-1651186).

References

- 1. Z. Gao, L. V. Mogni, E. C. Miller, J. G. Railsback, and S. A. Barnett, *Energy Environ. Sci.*, **9**, 1602 (2016).
- 2. S. Ji, I. Chang, Y. H. Lee, J. Park, J. Y. Paek, M. H. Lee, and S. W. Cha, *Nanoscale Res. Lett.*, **8**:48 (2013).
- 3. A. J. L. Reszka, R. C. Snyder, and M. D. Gross, *J. Electrochem. Soc.*, **161**, F1176 (2014).
- 4. M. Cottam, S. P. Muhoza, and M. D. Gross, J. Am. Ceram. Soc., 99, 2625 (2016).
- 5. S. P. Muhoza, M. A. Cottam, and M.D. Gross, *J. Vis. Exp.*, in press.
- 6. W. Wang, M. D. Gross, J. M. Vohs, and R. J. Gorte, *J. Electrochem. Soc.*, **154**, B439 (2007).
- 7. N. M. Vo and M. D. Gross, *J. Electrochem. Soc.*, **159**, B641 (2012).